

Two characteristic energies in the low-energy magnetic response of the electron-doped high-temperature superconductor $\text{Nd}_{2-x}\text{Ce}_x\text{CuO}_{4+\delta}$

G. Yu,^{1,2} Y. Li,^{1,*} E. M. Motoyama,¹ K. Hradil,³ R. A. Mole,⁴ and M. Greven^{2,5}¹*Department of Physics, Stanford University, Stanford, California 94305, USA*²*School of Physics and Astronomy, University of Minnesota, Minneapolis, Minnesota 55455, USA*³*Institut für Physikalische Chemie, Universität Göttingen, 37077 Göttingen, Germany*⁴*Forschungsneutronenquelle Heinz Maier-Leibnitz, 85747 Garching, Germany*⁵*Department of Applied Physics, Stanford University, Stanford, California 94305, USA*

(Received 10 September 2010; published 11 November 2010)

Neutron scattering for $\text{Nd}_{2-x}\text{Ce}_x\text{CuO}_{4+\delta}$ ($x \approx 0.155$, $T_c = 25$ K) reveals two distinct magnetic energy scales in the superconducting state: $\omega_1 \approx 6.4$ meV and $\omega_2 \approx 4.5$ meV. These magnetic energies agree *quantitatively* with the B_{1g}/B_{2g} and A_{1g} features observed in electronic Raman scattering, where the former is believed to indicate the maximum superconducting gap and the origin of the latter has remained unexplained. The data are inconsistent with previous claims of the existence of a magnetic resonance mode near 10 meV, but consistent with a resonance at ω_2 and with the recently established universal ratio of resonance energy to superconducting gap in unconventional superconductors [G. Yu *et al.*, *Nat. Phys.* **5**, 873 (2009)].

DOI: 10.1103/PhysRevB.82.172505

PACS number(s): 74.72.-h, 61.05.fg, 74.25.Ha, 75.40.Gb

Magnetic fluctuations might contribute to, or even be the cause of the superconductivity in the cuprates. The most prominent magnetic feature observed in the superconducting (SC) state is the *resonance*, an unusual spin-triplet ($S=1$) collective mode centered at the two-dimensional antiferromagnetic (AF) zone center $\mathbf{Q}_{\text{AF}}=(0.5,0.5)$ r.l.u.¹ The resonance has been observed in neutron-scattering experiments on a number of families of hole-doped cuprates: $\text{YBa}_2\text{Cu}_3\text{O}_{6+\delta}$ (Ref. 2) and $\text{Bi}_2\text{Sr}_2\text{CaCu}_2\text{O}_{8+\delta}$,³ which are comprised of two CuO_2 layers per unit cell, as well as in single-layer $\text{Tl}_2\text{Ba}_2\text{CuO}_{6+\delta}$ (Ref. 4) and $\text{HgBa}_2\text{CuO}_{4+\delta}$.⁵ The origin of the resonance and of its unusual dispersion has been a topic of much recent debate.^{1,6–11}

In recent years, an increasing number of magnetic neutron-scattering measurements have been carried out in the SC phase of the electron-doped cuprates. For $\text{Nd}_{2-x}\text{Ce}_x\text{CuO}_{4+\delta}$ (NCCO), such measurements have revealed a SC magnetic gap below T_c (Refs. 12 and 13) and evidence for sizable antiferromagnetic correlations.¹⁴ For $\text{Pr}_{0.88}\text{LaCe}_{0.12}\text{CuO}_4$ ($T_c=24$ K) (Ref. 15) and NCCO ($T_c=25$ K) (Ref. 16) an enhancement of the magnetic susceptibility $\chi''(\mathbf{Q}_{\text{AF}}, \omega)$ below T_c was found at $\omega \approx 10$ meV, which was interpreted as indicative of a magnetic resonance. This suggests that the resonance may be a universal feature of the cuprates, independent of the type of carriers.

In contrast to neutron scattering, which provides information about the magnetic degrees of freedom, electronic Raman scattering yields information about the charge dynamics. Polarization analysis has led to the identification of several characteristic energies in both hole- and electron-doped cuprates.^{17,18} Features observed in B_{1g} and B_{2g} symmetries have been associated with the normal-state pseudogap and the SC gap, respectively, whereas the unexpected observation of a feature in A_{1g} symmetry has found no widely accepted explanation. One suggestion for the hole-doped compounds is that the latter may be associated with the magnetic resonance.^{19–21}

In this Brief Report, we report a detailed magnetic

neutron-scattering study of NCCO near optimal doping (onset $T_c=25$ K). Upon cooling into the SC state, $\chi''(\mathbf{Q}_{\text{AF}}, \omega)$ exhibits a spectral weight shift from below to above $\omega_1 = 6.4(3)$ meV, which is best described as the opening of a gap at ω_1 and the concomitant emergence of additional spectral weight centered at $\omega_2 = 4.5(2)$ meV, below the gap. Remarkably, these two energies agree *quantitatively* with those obtained from Raman scattering in B_{1g}/B_{2g} and A_{1g} symmetries, respectively.¹⁸ The larger of the two corresponds to the maximum $2\Delta_{el}$ of the nonmonotonic electronic d -wave gap^{18,22} whereas the lower energy scale likely indicates the presence of a resonance, consistent with the situation for the hole-doped cuprates for which the resonance is always found below $2\Delta_{el}$. This conclusion is supported by two observations: (i) ω_2/ω_1 agrees with the universal ratio of resonance to gap energy found for a wide range of unconventional superconductors;²³ (ii) the temperature dependence of $\chi''(\mathbf{Q}_{\text{AF}}, \omega_2)$ exhibits an increase below T_c , as expected for the magnetic resonance. While the present results do not support the claim of a resonance at higher energies in NCCO,¹⁶ they lead to a universal picture of the resonance phenomenon²³ and point to a surprisingly simple connection between electronic and magnetic degrees of freedom in the electron-doped cuprates.

Two SC crystals were grown and prepared as described previously.^{24,25} The Ce concentration was carefully measured by inductively coupled plasma atomic emission spectrometry on several parts cut from the crystals and found to vary both along the diameter of the sample and along the growth direction. For the primary crystal used in this study (diameter: 4 mm; mass: 6.2 g), we estimate the overall composition to be $x=0.157(7)$. As discussed below, the chemical inhomogeneity manifests itself as a broadening of the features observed in our experiment. The value of T_c was determined from magnetic-susceptibility measurements of two small pieces (with compositions $x \approx 0.150$ and 0.164) cut from the ends of the crystal. Despite the somewhat different composition of the end pieces, the onset temperature of the transi-

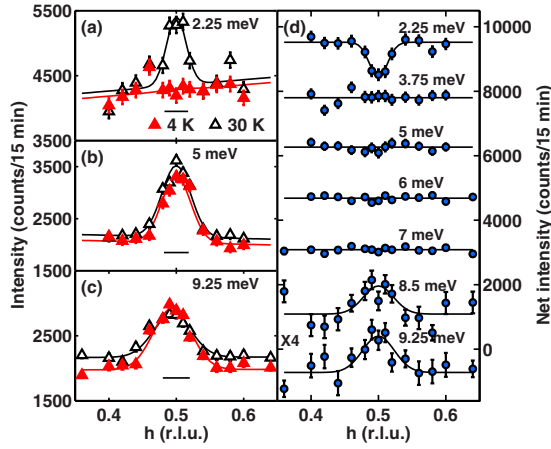


FIG. 1. (Color online) [(a)–(c)] Representative $[h, 1-h, 0]$ momentum scans through the AF zone center at $T=4$ and 30 K. The lines represent fits to a Gaussian. The horizontal bars indicate the resolution. (d) Intensity difference between $T=4$ and 30 K. For clarity, the data sets are shifted relative to each other by 1600 counts/15 min and the net intensities at $\omega=8.5$ and 9.25 meV are multiplied by a factor of 4.

tion is nearly the same, consistent with the maximum value of $T_c=25$ K generally obtained at and near optimal doping. The second crystal was smaller (mass: 5 g) and has a nearly identical composition [$x=0.156(4)$] and the same value of T_c .

The neutron-scattering experiment was performed on the thermal triple-axis instrument PUMA at the FRM-II in Garching, Germany. The two samples were mounted in separate measurements inside a low-temperature dispex such that the $(H, K, 0)$ plane was parallel to the horizontal scattering plane. We used a double-focusing pyrolytic graphite (PG)(002) monochromator, a focusing PG(002) analyzer, and a fixed final energy of 14.7 meV with a PG filter after the sample. The energy resolution ranged from about 0.8 to 1.4 meV [full width at half maximum (FWHM)] between $\omega = 1.5$ and 12 meV. The room-temperature lattice constants are $a=3.93$ Å and $c=12.08$ Å. Using a horizontally flat monochromator and analyzer, a rocking scan at the $(2,0,0)$ reflection indicated a mosaic of 0.3° (FWHM).

Figures 1(a)–1(c) show representative $[h, 1-h, 0]$ transverse momentum scans below (4 K) and above (30 K) T_c . At all energy transfers, the magnetic response remains centered at \mathbf{Q}_{AF} . Figure 1(a) demonstrates that at $\omega=2.25$ meV the normal-state response is resolution-limited and the magnetic scattering disappears completely deep in the SC state, indicating the opening of a gap. On the other hand, at $\omega=9.25$ meV, in addition to an overall change in background scattering, a clear enhancement at \mathbf{Q}_{AF} is observed in the SC state [Figs. 1(c) and 1(d)]. Between 3.75 and 7 meV, the intensity difference is featureless, as seen from Fig. 1(d).

Figure 2(a) reveals a clear intensity shift from below 4 to above 7 meV upon cooling. The peak susceptibility $\chi''_{AF}(\omega) \equiv \chi''(\mathbf{Q}_{AF}, \omega)$ at 4 and 30 K is obtained through a correction of the peak intensity by the Bose factor $[1 - \exp(-\hbar\omega/k_B T)]^{-1}$ [Fig. 2(b)]. Due to the increasing Bose factor difference between 4 and 30 K with decreasing energy, the

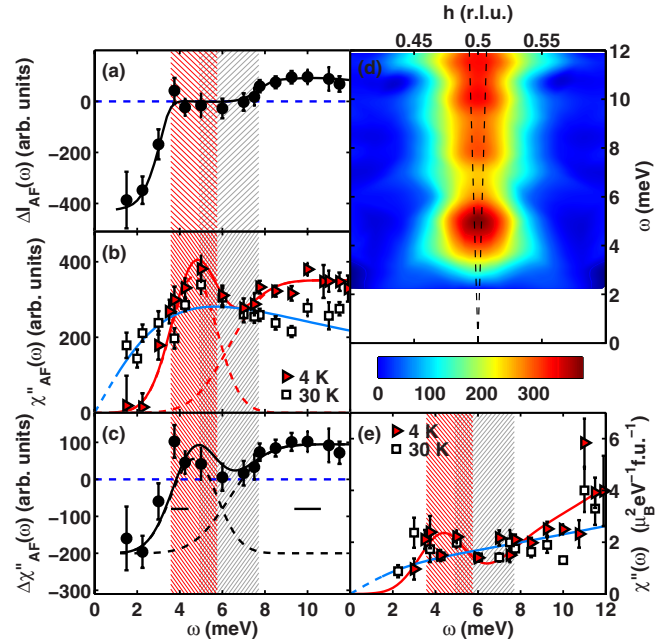


FIG. 2. (Color online) (a) Difference between $T=4$ and 30 K of the intensity amplitude at the antiferromagnetic wave vector \mathbf{Q}_{AF} . (b) Peak susceptibility $\chi''_{AF}(\omega)$, obtained by correcting the measured peak intensity for the Bose factor. (c) Relative change in $\chi''_{AF}(\omega)$ between $T=4$ and 30 K. (d) Contour plot of $\chi''(\mathbf{Q}, \omega)$ at 4 K, made by interpolation of symmetrized momentum scans of the kind shown in Figs. 1(a)–1(c) with a constant background removed. (e) Local susceptibility, obtained in absolute units from the momentum integral of $\chi''(\mathbf{Q}, \omega)$ by comparing with the measured intensity of acoustic phonons. The continuous lines in (a) and (e) are guides to the eyes while the lines in (b) and (c) are the results of fits, as described in the text. The horizontal bars in (c) indicate the FWHM energy resolution of 0.9 meV and 1.25 meV at $\omega=4$ meV and 10 meV, respectively. The shaded vertical bands centered at about 4.5 and 6.5 meV indicate the respective ranges of A_{1g} and B_{1g} peak energies from Raman scattering (Ref. 18) corresponding to the chemical inhomogeneity in our sample. The inelastic neutron scattering data were obtained during two separate experimental runs. Peak intensities and susceptibilities were obtained from Gaussian fits. The energy dependence of the intrinsic momentum width is approximately linear above 4 meV with a slope of 320(30) meV Å and indistinguishable between 4 K and 30 K. Assuming a cone of spin-wavelike excitations, we estimate the corresponding velocity to be 175(50) meV Å, significantly smaller than the spin-wave velocity of about 1 eV Å in undoped Nd_2CuO_4 [dashed line in (d)] (Ref. 26).

observed zero (within error) net peak intensity between 3.75 and 7 meV [Fig. 1(d)] directly leads to a local maximum in the susceptibility difference around 4 meV at 4 K. The normal-state response at 30 K is well described by a Lorentzian, $\chi''_{AF}(\omega) = \chi''_{AF} \Gamma \omega / (\Gamma^2 + \omega^2)$, with relaxation rate $\Gamma = 5.7(5)$ meV. In contrast, the excitation spectrum in the SC state exhibits two characteristic energies: a local maximum at 4–5 meV and a minimum at 6–7 meV. This can also be seen from the susceptibility difference in Fig. 2(c) and from the low-temperature contour plot in Fig. 2(d). Our measurement of the temperature dependence of $\chi''_{AF}(\omega)$ provides further evidence that the local maximum at 4.5 meV is physical and

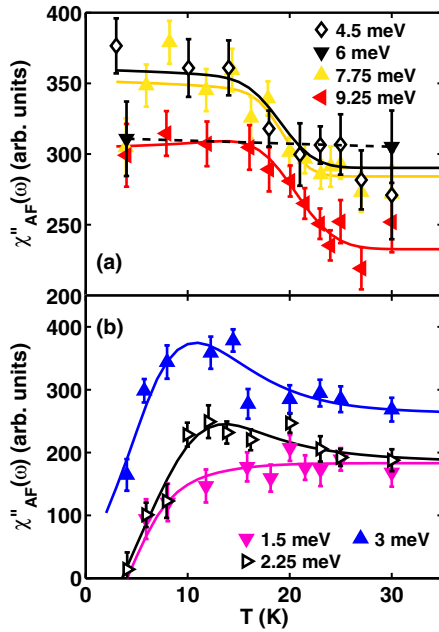


FIG. 3. (Color online) Temperature dependence of the peak susceptibilities at (a) $\omega=9.25, 7.75, 6,$ and 4.5 meV and (b) $\omega=3, 2.25,$ and 1.5 meV. The result at 4.5 meV represents the combined statistics of data at $\omega=4$ and 5 meV obtained for a second crystal with the same T_c and nearly identical composition. The dashed line indicates a linear interpolation of the 6 meV data.

distinct from the feature above 7 meV [Fig. 3(a)], since an enhancement of peak susceptibility right below T_c is observed at both 4.5 and above 7.75 meV, but not at 6 meV.

Raman-scattering results for both NCCO and $\text{Pr}_{2-x}\text{Ce}_x\text{CuO}_{4+\delta}$ (Ref. 18) demonstrate a nearly linear decrease above $x \approx 0.15$ of the energy scales in B_{1g} , B_{2g} , and A_{1g} symmetries. Unlike for the hole-doped compounds, the characteristic energies in B_{1g} and B_{2g} symmetries are nearly identical, suggesting that in both cases one effectively measures the maximum SC gap $2\Delta_{el}$ at the intersection of the Fermi surface with the AF Brillouin zone, in between nodal and antinodal directions.^{18,22} The chemical composition of our main NCCO sample ranges from $x=0.150$ to 0.164 , which corresponds to a range of about 3 meV of these two energy scales, as indicated by the two vertical bands in Fig. 2. These ranges are in good agreement with the positions of the extrema in the low-temperature magnetic susceptibility. In order to quantify this observation of a correspondence of magnetic and electronic energy scales, we describe the 4 K data for $\chi''_{AF}(\omega)$ in Fig. 2(b) by a step function for the electronic gap, centered at $\omega_1 = \omega_{B_{1g}}$, plus a Gaussian excitation below the gap, centered at $\omega_2 = \omega_{A_{1g}}$. The widths of the two features are fixed, chosen to correspond to a (Gaussian) broadening due to the Ce inhomogeneity, and *the fit therefore contains only two adjustable parameters*: the amplitudes of the Gaussian [$A_G=363(18)$ (arb. units)] and of the step function [$A_S=351(8)$ (arb. units)]. As can be seen from Fig. 2(b), $\chi''_{AF}(\omega)$ in the SC state is described in an excellent fashion based on the knowledge of electronic energy scales from Raman scattering and the sample inhomogeneity from chemical analysis. A similarly good fit is obtained for the

difference data in Fig. 2(c). We note that a separate five-parameter fit of the $T=4$ K data in Fig. 2(b) yields $\omega_1 = 6.4(3)$ meV, $\omega_2 = 4.5(2)$ meV, and a Gaussian broadening of $\Gamma = 2.7(3)$ meV (FWHM).

The magnetic response upon entering the SC state consists of two components: a broad rearrangement of spectral weight from low energies to energies above ω_1 and an additional new component centered at ω_2 . We consider two possible explanations for this second energy scale: it could either be related to the observation of a nonmonotonic d -wave gap^{18,22} or it may be the magnetic resonance. The nonmonotonic d -wave gap is characterized by a maximum away from the antinodal direction. Photoemission work on $\text{Pr}_{1-x}\text{LaCe}_x\text{CuO}_{4+\delta}$ near optimal doping suggests that the antinodal gap value is approximately 80% of the maximum gap, and our data give $\omega_2/\omega_1 = 70(4)\%$. However, it seems unlikely that a significant contribution to the low-energy magnetic response stems from the antinodal regions, since they are not spanned by the wave vector \mathbf{Q}_{AF} .²⁷

On the other hand, the low-energy feature may be the magnetic resonance. Figure 3(a) demonstrates that a continuous enhancement of $\chi''_{AF}(\omega)$ upon cooling into the SC state already exists around $\omega=4.5$ meV. While our data are overall consistent with Refs. 15 and 16, these earlier results were interpreted as indicative of a resonance mode at $\omega_r = 9.5\text{--}11$ meV. This conclusion was supported by the observation that the ratio $\omega_r/k_B T_c \approx 5$ is in good agreement with results for hole-doped cuprates. However, for NCCO, the interpretation of the susceptibility enhancement around 10 meV as the resonance is unphysical and inconsistent with the fact that the resonance in the hole-doped compounds lies below $2\Delta_{el}$.¹ Moreover, recent work for $\text{HgBa}_2\text{CuO}_{4+\delta}$ revealed that the ratio $\omega_r/k_B T_c$ is not universal.⁵ Instead, a universal relation $\omega_r \approx 0.64 \times 2\Delta_{el}$ has been observed for several types of unconventional superconductors, including the hole-doped cuprates.²³ The presence of a magnetic resonance in NCCO at about 70% of $2\Delta_{el}$ is consistent with this universal behavior.

Recent scanning tunneling microscopy (STM) work on $\text{Pr}_{0.88}\text{LaCe}_{0.12}\text{CuO}_{4+\delta}$ ($T_c=24$ K) (Ref. 28) indicated that $2\Delta_{el} \approx 14$ meV, significantly larger than in NCCO.^{18,29} Therefore, while our results are inconsistent with the existence of a resonance near 10 meV in NCCO,¹⁶ they are not necessarily inconsistent with the original observations of Ref. 15. It will be important to confirm the observation of a relatively large electronic gap in $\text{Pr}_{0.88}\text{LaCe}_{0.12}\text{CuO}_{4+\delta}$ with other experimental methods. Furthermore, STM revealed a bosonic mode at about 10.5 meV, consistent with the enhancement of magnetic susceptibility around 10 meV in $\text{Pr}_{0.88}\text{LaCe}_{0.12}\text{CuO}_{4+\delta}$.²⁸ If the bosonic mode is indeed magnetic in origin, STM should locate it at ω_2 in optimally doped NCCO.

The interpretation of the ω_2 feature as the resonance implies that the resonance energy agrees well with the Raman A_{1g} response, consistent with the suggestion for the hole-doped compounds that the latter may be associated with the magnetic resonance.^{19–21}

Figure 3(b) reveals a nontrivial nonmonotonic temperature dependence at lower energies. The enhancement of $\chi''_{AF}(\omega)$ at $\omega=4.5$ meV and the nonmonotonic temperature

dependence at $\omega=2.25$ and 3 meV appear to be the joint effect of the opening of the gap and the formation of a new excitation below $2\Delta_{el}$ in the SC state. We note that the interpretation of the low-energy response in terms of a gap and an in-gap excitation requires a reinterpretation of the results of Refs. 12 and 13 in which the low-energy edge of the magnetic susceptibility in the SC state was directly associated with a gap.

Figure 2(e) shows the local susceptibility, $\chi''(\omega) = \int dQ^3 \chi''(Q, \omega) / \int dQ^3$. In the normal state, $\chi''(\omega)$ increases monotonically from zero at $\omega=0$ meV to about $2.5\mu_B^2$ eV⁻¹ f.u.⁻¹ at 12 meV. In the SC state, $\chi''(\omega)$ exhibits a local maximum of $\approx 2\mu_B^2$ eV⁻¹ f.u.⁻¹ at ω_2 and reaches $\approx 4\mu_B^2$ eV⁻¹ f.u.⁻¹ at 12 meV. The estimated mean-square fluctuating moment $\langle m^2 \rangle = \int d\omega \chi''(\omega)$ integrated up to 12 meV is $0.019\mu_B^2$ f.u.⁻¹ and $0.021\mu_B^2$ f.u.⁻¹ at 30 K and 4 K, respectively. Although the difference is only 10%, the trend seen from the data indicates that integration somewhat beyond 12 meV would lead to a larger difference. Unfortunately, the regime just above 12 meV is inaccessible due to high background scattering from Nd³⁺ crystal-field excitations. This suggests that the susceptibility enhancement above ω_1 and the ω_2 feature cannot both be compensated for by the low-energy spectral-weight loss in the superconducting state and that some high-energy (above 12 meV) spectral weight must shift to lower energy to satisfy the total moment sum rule. If the $\omega_2 \approx 4$ meV feature were not present, the superconductivity-induced local-susceptibility enhancement

above ω_1 ($\approx 0.004\mu_B^2$ f.u.⁻¹ up to 12 meV) would be fully covered by the spectral-weight depletion in the gap ($\approx 0.007\mu_B^2$ f.u.⁻¹). We estimate the momentum- and energy-integrated weight of the low-energy feature to be $0.007(2)\mu_B^2$ f.u.⁻¹. This value is somewhat smaller (by a factor of 3–10) than the weight of the resonance in the hole-doped compounds.¹

While the magnitude of $\chi''(\omega)$ is consistent with work on Pr_{0.88}LaCe_{0.12}CuO_{4+ δ} ,^{15,30} the SC and normal-state responses [both $\chi''(\omega)$ and $\chi''_{AF}(\omega)$] of the latter system do not approach zero at low energies. The magnetic gap is an expected feature of the excitation spectrum, and it is also observed in hole-doped YBa₂Cu₃O_{6+ δ} (Ref. 31) and La_{2- x} Sr _{x} CuO₄ (Ref. 32) near optimal doping. We speculate that, as in early measurements on hole-doped La_{2- x} Sr _{x} CuO₄,³³ disorder effects might mask the underlying low-energy response of Pr_{1- x} LaCe _{x} CuO_{4+ δ} .

In summary, careful analysis of new neutron-scattering data for electron-doped Nd_{2- x} Ce _{x} CuO_{4+ δ} reveals quantitative agreement for the low-energy magnetic response at the antiferromagnetic wave vector with electronic energy scales from Raman scattering. The larger of the two magnetic energies corresponds to the electronic-gap maximum while the smaller scale is likely the magnetic resonance.

This work was supported by the DOE under Contract No. DE-AC02-76SF00515 and by the NSF under Grant. No. DMR-0705086.

*Present address: Max Planck Institute for Solid State Research, 70569 Stuttgart, Germany.

¹M. Eschrig, *Adv. Phys.* **55**, 47 (2006).

²J. Rossat-Mignod *et al.*, *Physica C* **185-189**, 86 (1991).

³H. F. Fong *et al.*, *Nature (London)* **398**, 588 (1999).

⁴H. He *et al.*, *Science* **295**, 1045 (2002).

⁵G. Yu *et al.*, *Phys. Rev. B* **81**, 064518 (2010).

⁶E. W. Carlson *et al.*, *Phys. Rev. B* **70**, 064505 (2004).

⁷F. Krüger and S. Scheidl, *Phys. Rev. B* **70**, 064421 (2004).

⁸I. Sega and P. Prelovšek, *Phys. Rev. B* **73**, 092516 (2006); P. Prelovšek and I. Sega, *ibid.* **74**, 214501 (2006).

⁹G. Seibold and J. Lorenzana, *Phys. Rev. B* **73**, 144515 (2006).

¹⁰G. S. Uhrig *et al.*, *Phys. Rev. Lett.* **93**, 267003 (2004).

¹¹M. Vojta *et al.*, *Phys. Rev. Lett.* **97**, 097001 (2006).

¹²K. Yamada *et al.*, *Phys. Rev. Lett.* **90**, 137004 (2003).

¹³E. M. Motoyama *et al.*, *Phys. Rev. Lett.* **96**, 137002 (2006).

¹⁴E. M. Motoyama *et al.*, *Nature (London)* **445**, 186 (2007).

¹⁵S. D. Wilson *et al.*, *Nature (London)* **442**, 59 (2006).

¹⁶J. Zhao *et al.*, *Phys. Rev. Lett.* **99**, 017001 (2007).

¹⁷T. P. Devereaux and R. Hackl, *Rev. Mod. Phys.* **79**, 175 (2007).

¹⁸M. M. Qazilbash *et al.*, *Phys. Rev. B* **72**, 214510 (2005).

¹⁹Y. Gallais *et al.*, *Phys. Rev. Lett.* **88**, 177401 (2002).

²⁰M. Le Tacon *et al.*, *Phys. Rev. B* **71**, 100504(R) (2005).

²¹M. Le Tacon *et al.*, *J. Phys. Chem. Solids* **67**, 503 (2006).

²²H. Matsui *et al.*, *Phys. Rev. Lett.* **95**, 017003 (2005).

²³G. Yu *et al.*, *Nat. Phys.* **5**, 873 (2009).

²⁴P. K. Mang *et al.*, *Phys. Rev. Lett.* **93**, 027002 (2004).

²⁵P. K. Mang *et al.*, *Phys. Rev. B* **70**, 094507 (2004).

²⁶P. Bourges *et al.*, *Phys. Rev. Lett.* **79**, 4906 (1997).

²⁷N. P. Armitage *et al.*, *Phys. Rev. Lett.* **88**, 257001 (2002).

²⁸F. C. Niestemski *et al.*, *Nature (London)* **450**, 1058 (2007).

²⁹S. Kashiwaya *et al.*, *Phys. Rev. B* **57**, 8680 (1998).

³⁰F. Krüger *et al.*, *Phys. Rev. B* **76**, 094506 (2007).

³¹P. Bourges *et al.*, *Science* **288**, 1234 (2000); P. Dai *et al.*, *Phys. Rev. B* **63**, 054525 (2001).

³²K. Yamada *et al.*, *Phys. Rev. Lett.* **75**, 1626 (1995).

³³See Ref. 32, and references therein.